

# Evolution of Nagaoka phase with kinetic energy frustrating hoppings

F. T. Lisandrini,<sup>1</sup> B. Bravo,<sup>2</sup> A. E. Trumper,<sup>1</sup> L. O. Manuel,<sup>1</sup> and C. J. Gazza<sup>1</sup>

<sup>1</sup>*Instituto de Física Rosario (CONICET) and Universidad Nacional de Rosario,  
Bvd. 27 de Febrero 210 bis, (2000) Rosario, Argentina*

<sup>2</sup>*Instituto de Física de La Plata, UNLP-CONICET and Departamento de Física,  
Facultad de Ciencias Exactas, Universidad Nacional de La Plata, 1900 La Plata, Argentina.*

(Dated: February 3, 2017)

We investigate, using the density matrix renormalization group, the evolution of the Nagaoka state with  $t'$  hoppings that frustrate the hole kinetic energy in the  $U = \infty$  Hubbard model on the anisotropic triangular lattice and the square lattice with second-nearest neighbor hoppings. We find that the Nagaoka ferromagnet survives up to a rather small  $t'_c/t \sim 0.2$ . At this critical value, there is a transition to an antiferromagnetic phase, that depends on the lattice: a  $\mathbf{Q} = (Q, 0)$  spiral order, that continuously evolves with  $t'$ , for the triangular lattice, and the usual  $\mathbf{Q} = (\pi, \pi)$  Néel order for the square lattice. Remarkably, the local magnetization takes its classical value for all considered  $t'$  ( $t'/t \leq 1$ ). Our results show that the recently found classical kinetic antiferromagnetism, a perfect counterpart of Nagaoka ferromagnetism, is a generic phenomenon in these kinetically frustrated electronic systems.

**PACS numbers:** 75.10.Lp, 71.10.Fd

## I. INTRODUCTION

Nagaoka's theorem<sup>1</sup> stands almost alone as a rigorous result about itinerant magnetism. It predicts the existence of a fully polarized ferromagnetic state as the unique ground state of the  $U = \infty$  Hubbard model, when one hole is doped away half-filling and certain connectivity conditions are satisfied. Despite its very restricted validity and its thermodynamic irrelevance, the theorem introduced an interesting idea about quantum magnetism: kinetic magnetism, the possibility of magnetic order driven solely by the motion of the electrons.

Since the seminal work by Nagaoka<sup>1</sup>, a lot of effort has been dedicated to the study of Nagaoka ferromagnetism stability beyond the constraints of the theorem. In particular, some controversy arose as to whether the fully polarized state survives for a finite density of holes (see<sup>2-4</sup> and references therein). However, large-scale density matrix renormalization group (DMRG) calculations<sup>5</sup>, among others<sup>4,6,7</sup> seem to have solved the problem, unless for the square lattice, as they predict the existence of Nagaoka ferromagnetism up to critical hole density  $\delta_c \simeq 0.2$ . Little is known about the states that supplant the Nagaoka ferromagnet beyond  $\delta_c$ <sup>5,7</sup>.

With respect to the  $U = \infty$  condition, its relaxation leads to the competition between the Nagaoka and antiferromagnetic exchange mechanisms. This entails the instability of the Nagaoka phase against phase separation: for  $U/t \lesssim 130$ , a ferromagnetic polaron around the hole moves on an antiferromagnetic background<sup>8</sup>.

Lastly, the violation of the connectivity condition<sup>4,9</sup> can also destabilize the Nagaoka phase. Nagaoka's theorem requires that  $S_{loop} = 1$ , where  $S_{loop}$  is the sign of the hopping amplitudes around the smallest loop of the lattice. When this condition is not fulfilled the hole kinetic energy is frustrated. Kinetic frustration<sup>10-12</sup> is a quantum mechanical phenomenon, without classical analog

since it originates in the quantum interferences of different hole paths. A simple way to break the connectivity condition is the consideration of particular signs for the hopping parameters in non-bipartite lattices. As an alternative way, the hopping integrals can be modulated by a staggered magnetic flux<sup>12</sup>.

In 2005, Haerter and Shastry<sup>13</sup> found that the ground state of the  $U = \infty$  triangular Hubbard with  $t > 0$ , a kinetically frustrated system where Nagaoka's theorem is not valid ( $S_{loop} = -1$ ), has a  $120^\circ$  Néel order. More recently, we found another example of kinetic antiferromagnetism, a  $(\pi, \pi)$  Néel order as the ground state of the square Hubbard model with second-nearest neighbor hopping  $t' = t > 0$ , and we uncovered the classical nature of these antiferromagnets<sup>14</sup>. At the same time, we proposed a microscopic mechanism responsible for this kinetic antiferromagnetism, based on the relaxation of the kinetic frustration as the hole moves on an antiferromagnetic background.

In order to deepen our understanding of kinetic magnetism, in this work we study the evolution of the Nagaoka ferromagnet with kinetically frustrating  $t'$  hoppings. To make it, we solve the  $U = \infty$  Hubbard model on the anisotropic triangular lattice and the square lattice with second-nearest neighbor hopping (see Fig. 1), using the numerically exact DMRG. As we vary  $t'$  we can move between the two known limits: the Nagaoka state ( $t' = 0$ ) and the novel kinetic antiferromagnet ( $t' = t$ )<sup>14</sup>. We find that the classical order extends for all  $t'$ , ferromagnetic below a critical  $t'_c$  (that slightly depends on the lattice), and antiferromagnetic above. We analyze the characteristics of the transition, the antiferromagnetic structure above  $t'_c$ , and the physical microscopic mechanism at work for each lattice.

Beyond the sustained theoretical interest in kinetic magnetism for decades, up to date, there are no clear experimental realization of Nagaoka conditions. At the

end of this work, we briefly mention some recent experimental proposals.

## II. MODEL AND METHOD

In order to analyze the stability of the Nagaoka ferromagnetic state against kinetic frustration, we study the  $U = \infty$  Hubbard model, with one hole doped away the half-filled case, on two lattices: the spatially anisotropic triangular lattice and the square lattice with second-nearest neighbor hoppings, as shown in Fig. 1. The Hubbard model reads

$$\hat{H} = - \sum_{ij\sigma} t_{ij} \hat{c}_{i\sigma}^\dagger \hat{c}_{j\sigma} + U \sum_i \hat{n}_{i\uparrow} \hat{n}_{i\downarrow}, \quad (1)$$

where  $i, j$  denote pair of sites on each lattice,  $t_{ij}$  are the hopping integrals, and  $U$  is the onsite Coulomb repulsion. In Fig. 1, the solid lines represent  $t$  (which we take as the energy scale,  $t = 1$ ), while the dashed lines represent  $t'$ , the varying anisotropic hoppings (second-nearest neighbor hoppings) for the triangular (square) lattice. It should be noticed that, for  $t' = 0$ , the Hubbard model on the two lattices are equivalent. When  $t' = 0$ , the connec-

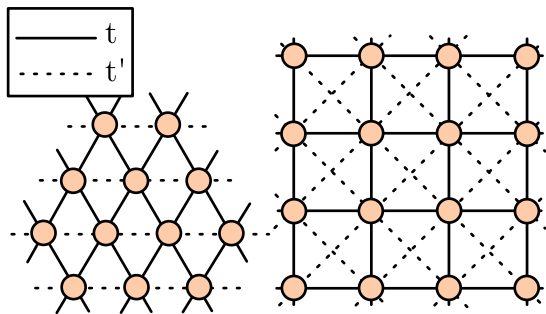


FIG. 1. Triangular lattice with spatially anisotropic hoppings and square lattice with second-nearest neighbor hoppings.  $t'$ s are the kinetically frustrating hoppings. We take  $t = 1$  as the energy unit.

tivity condition of Nagaoka's theorem is fulfilled because the minimal loops for the hole motion are squares with  $\mathbb{S}_{loop} = \text{sgn}(-t)^4 = +1$ . For finite  $t'$ , the minimal loops are triangles with  $\mathbb{S}_{loop} = \text{sgn}(-t')(-t)^2 = -\text{sgn}(t')$ . So, for  $t' \leq 0$ , the theorem is valid and the ground state is a unique fully polarized ferromagnetic state for both lattices. On the other hand, a positive  $t'$  introduces kinetic energy frustration in the hole motion ( $\mathbb{S}_{loop} = -1$ ), invalidating Nagaoka's theorem. In a previous work<sup>14</sup>, we have shown that, in the special case  $t' = t$ , the ground states have classical antiferromagnetic orders: a  $120^\circ$  pattern for the (isotropic) triangular lattice and the usual  $\mathbf{Q} = (\pi, \pi)$  for the square one.

In this work we will use DMRG<sup>15,16</sup> to solve the ground state of the  $U = \infty$  Hubbard model, for  $0 \leq t' \leq 1$ . We apply DMRG to ladders of dimension  $L_x \times L_y$ ,

with  $L_y = 6$  legs (enough to describe correctly two-dimensional systems<sup>5</sup>) and up to  $L_x = 15$  rungs. We impose cylindrical boundary conditions with periodic wrapping in the rung direction and open boundary conditions along the legs. To maintain errors of the DMRG smaller than symbol sizes in each figure, we have kept up to  $m = 500$  states, with a truncation error less than  $O(10^{-7})$ .

## III. RESULTS

### A. Ground state energy and critical $t'_c$

As we mentioned above, the  $t' = 0$  ground state of Hamiltonian (1) is ferromagnetic, while for  $t' = t$  it exhibits antiferromagnetic order for each lattice<sup>14</sup>. Hence, there will be a critical value  $t'_c$  where the Nagaoka state is destabilized. To determine  $t'_c$ , we have resorted to an energy analysis. Let  $E_N(S^z)$  be the ground state energy of the  $U = \infty$  Hubbard model, for an  $N$ -site lattice (with  $N - 1$  electrons) and a given sector of the spin projection  $S^z$ . For a given  $t'$ , we have compared the (ground state) energies of the different spin projection sectors, from the maximal  $S_{max}^z = \frac{N-1}{2}$ —corresponding to a full spin polarization in the  $z$  direction—to the minimal  $S_{min}^z = \frac{1}{2}$ . Notice that, due to the  $SU(2)$  symmetry of the model, the ferromagnetic Nagaoka state is  $2S_{max} + 1$ -fold degenerate, where  $S_{max} = \frac{N-1}{2}$  is its total spin, and it has projections in all the  $S^z$  sectors.

We have found that, for small values of  $t'$  and for both lattices, the computed ground state energies of all the  $S^z$  sectors are degenerate (in particular,  $E_N(S_{min}^z) = E_N(S_{max}^z)$ ). Therefore, we can suspect that these degenerate states belong to the Nagaoka ground state manifold. As a check, we have verified that the spin correlations, for different  $S^z$  sectors, correspond to a fully saturated ferromagnet ( $\langle \mathbf{S}_i \cdot \mathbf{S}_j \rangle \simeq \frac{1}{4}$  for  $i \neq j$ ), discarding then the possibility that the Nagaoka state may be degenerate with lower total spin states. On the other hand, for larger values of  $t'$ , we have obtained that the ground state always belongs to the minimal spin projection sector  $S_{min}^z$ , which would correspond to a total spin  $S = \frac{1}{2}$ . We have not found partially polarized ground states for any  $t'$ , although we must warn that, very close to the transition point  $t'_c$ , the flattening of  $E_N(S^z)$  makes the numerical treatment harder and less precise. With this caveat, we can say that, at  $t'_c$ , there will be a transition from a Nagaoka ferromagnet to a minimal spin state which, later on, we will characterize as an antiferromagnetic state. To determine the critical  $t'_c$ , firstly we have looked for the  $t'$  value where the degeneracy between  $E_N(S_{min}^z)$  and  $E_N(S_{max}^z)$  is broken for each lattice. In Figs. 2 and 3 we show these energies as a function of  $t'$  and for different cluster sizes, for the triangular and square lattices, respectively. We can see that the degeneracy is broken in the region around  $t' \sim 0.2 - 0.3$ , signaling, as we explained above, that the ground state of the systems

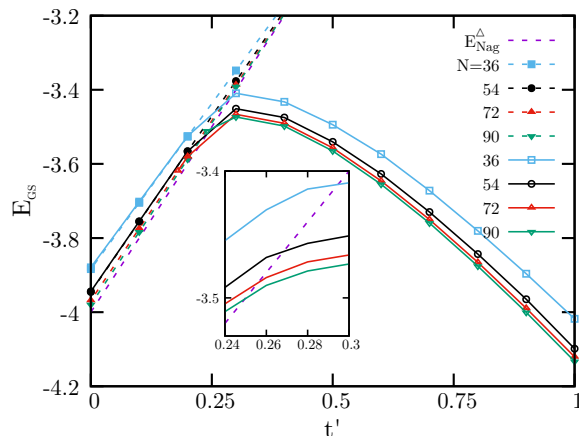


FIG. 2. Ground state energy  $E_N(S^z)$  for the triangular lattice as a function of  $t'$ , and for different  $N$ -site clusters. Dashed (solid) lines correspond to the  $S^z = S_{max}^z$  ( $S_{min}^z$ ) sector energy. For smaller  $t'$  both energies overlap.  $E_{Nag}^{\Delta}$  is the thermodynamic limit of the Nagaoka state energy. Inset: zoom of the critical region, showing the intersection of  $E_N(S_{min}^z)$  with the ferromagnetic energy  $E_{Nag}^{\Delta}$ .

$N$	18	36	54	72	90	$\infty$
$t_c^{\Delta}$	0.387	0.295	0.268	0.256	0.249	0.222

TABLE I. Critical  $t'_c$  values for different  $N$ -site triangular clusters, and its  $N \rightarrow \infty$  extrapolation limit.

moves from the highest-spin Nagaoka state to another one with minimal total spin.

As the conventional DMRG algorithm uses the  $S^z$  quantum number without discriminating between different total spin  $S$ , we cannot compute the energy of the excited  $S = \frac{1}{2}$  state below  $t'_c$  (notice that, in this case, the calculated  $E_N(S_{min}^z)$  corresponds to the  $S^z = \frac{1}{2}$  sector energy of the  $S_{max}$  Nagaoka ground state). Therefore, we do not have access to the expected energy level crossing between the highest- and lowest-spin sectors, that would facilitate the determination of  $t'_c$ . For the square lattice model, the lack of the level crossing is not so important as there is an appreciable kink in the ground state energy at  $t'_c$  (see main panel of Fig. 3). However, for the triangular case, the transition seems to be much smoother, as is shown in the main panel of Fig. 2, and, consequently, it is more difficult to estimate the critical point where the degeneracy between  $E_N(S_{max}^z)$  and  $E_N(S_{min}^z)$  is lost. To avoid this difficulty, we have evaluated  $t'_c$  extrapolating the level crossing between  $E_N(S_{min}^z)$  and the infinite-lattice Nagaoka energy,  $E_{Nag}$  (see insets of Figs. 2 and 3).  $E_{Nag}$  can be computed exactly as the problem of one hole moving in a ferromagnetic background is identical to the spinless tight-binding system<sup>17</sup>

First, we consider the anisotropic triangular lattice.

$N$	24	36	48	60	72	84	$\infty$
$t_c^{\square}$	0.256	0.232	0.225	0.220	0.218	0.217	0.214

TABLE II. Critical  $t'_c$  for different  $N$ -site square clusters, and its  $N \rightarrow \infty$  extrapolation limit.

The corresponding Nagaoka ground state energy is,  $E_{Nag}^{\Delta} = -4|t| + 2t'$ , which is shown in Fig. 2 with the DMRG results. Following the procedure mentioned above, in Table I we give the critical  $t_c^{\Delta}$  hoppings for different  $N$ -site clusters. We have extrapolated these values assuming that  $t'_c \propto 1/N^2$ , and we have obtained  $t_c^{\Delta} \simeq 0.222$  in the thermodynamic limit.

Second, for the square lattice with second-nearest neighbor hoppings, the exact energy of the fully polarized state in the thermodynamic limit is,  $E_{Nag}^{\square} = -4|t| + 4t'$ , (with  $t' < 0.5$ ) and it is shown in Fig. 3. In Table II we present the critical values for different  $N$ -site clusters, leading to  $t_c^{\square} \simeq 0.214$  in the  $N \rightarrow \infty$  limit. This value is quite close to the only one that existed in the literature up to the present,  $t_c \simeq 0.255$ , obtained within a restricted Hilbert space<sup>9</sup>.

It is instructive to compare our results with the solution of the simplest systems that preserve the basics of Nagaoka physics. That is, three electrons in Hubbard square four-site clusters with nearest-neighbor  $t$  hoppings and (a)  $t'$  hopping along only one diagonal (triangular lattice); (b)  $t'$  hoppings along both diagonals (square lattice)<sup>4</sup>. In both cases, there is an energy level crossing for some  $t'_c$ . For  $t' < t'_c$  the ground state has  $S = \frac{3}{2}$ , corresponding to the Nagaoka state, while for  $t' > t'_c$ , the ground state has minimal spin  $S = \frac{1}{2}$ . For system (a) the

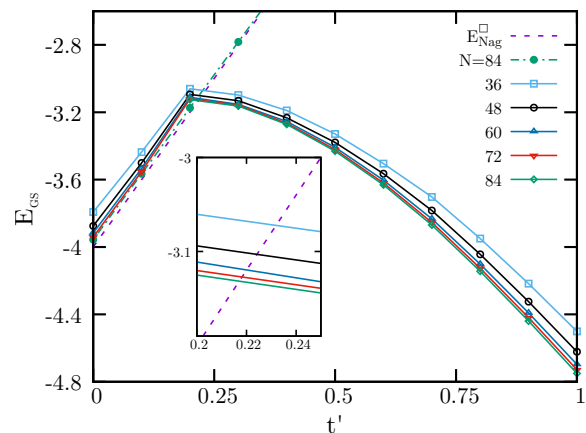


FIG. 3. Ground state energy  $E_N(S_z)$  for the square lattice as a function of  $t'$ , and for different  $N$ -site clusters. Dashed (solid) lines correspond to the  $S_z = S_{max}^z$  ( $S_z = \frac{1}{2}$ ) sector energy.  $E_{Nag}^{\square}$  is the thermodynamic limit of the Nagaoka state energy. Inset: zoom of the critical region, showing the intersection of  $E_N(\frac{1}{2})$  with the ferromagnetic energy  $E_{Nag}^{\square}$ .

transition occurs at  $t'_c/t = \frac{1}{\sqrt{14}} \simeq 0.267$ , while for system (b)  $t'_c/t = 0.25$ . These values roughly correspond to the gap energy  $\Delta$  between the  $S = \frac{3}{2}$  and  $S = \frac{1}{2}$  ground states for  $t' = 0$ , that is,  $\Delta = (2 - \sqrt{3})t \simeq 0.267t$ . It is remarkable that the critical  $t'_c$  values for these toy models are very close to the thermodynamic limit ones that we have presented above (Tables I and II). From this fact, we can deduce that the relevant quantum interferences for the Nagaoka physics are those associated with the hole motion along the smallest lattice loops.

We want to draw attention to the fact that the critical hoppings for both lattices are very similar ( $t'_c^\Delta \simeq 0.222$ ,  $t'_c^\square \simeq 0.214$ ), and also they are numerically similar to the critical doping for the destabilization of the Nagaoka state for  $t' = 0$ , that is,  $\delta_c \simeq 0.2^{5,6}$ . We guess that this agreement is not casual: if the Nagaoka ferromagnet, with  $t' = 0$  and one hole doped, is separated by an energy gap  $\Delta$  of other spin sectors, it is plausible that a ‘‘perturbation’’ may destabilize the phase as long as its characteristic energy is of the order of  $\Delta$  (In the case of doping, we can associate it with an energy  $\varepsilon \propto \delta \times t$ ). So, if this argument is correct, we expect a gap of the order of  $0.2t$  for the  $t' = 0$  Nagaoka ferromagnet in the square lattice, a value close to the gap for the 4-site cluster system.

## B. Magnetic wave vector

The magnetic properties of the ground state can be inferred from the static magnetic structure factor  $\mathcal{S}(\mathbf{k})$  defined as

$$\mathcal{S}(\mathbf{k}) = \frac{1}{N} \sum_{ij} \langle \mathbf{S}_i \cdot \mathbf{S}_j \rangle e^{i\mathbf{k}(\mathbf{R}_i - \mathbf{R}_j)}, \quad (2)$$

where  $i, j$  run over all sites. We evaluate  $\mathcal{S}(\mathbf{k})$  for  $\mathbf{k} \in [0, 2\pi) \otimes [0, 2\pi)$ , since all the momenta that belong to the first Brillouin zone of each lattice have an equivalent point in this region; for reference, the edges of the Brillouin zones will be displayed in the figures. The  $k_y$  component of each momentum is unequivocally determined by the periodic boundary conditions along the  $y$  direction; on the other hand, the open boundary conditions along the  $x$  direction do not impose any restriction for the  $k_x$  component. Therefore, we can take advantage of this freedom to circumvent the discreteness of  $\mathbf{k}$  in the  $x$  direction.

We have observed that  $\mathcal{S}(\mathbf{k})$  exhibits a pronounced peak for a certain momentum (and equivalent points in the reciprocal space), for both lattices, and all  $t'$ , except very close to the critical  $t'_c$ , as we will discuss later. The intensity of the peak increases linearly with the cluster size, pointing out the existence of long-range magnetic order, and its position determines the magnetic wave vector  $\mathbf{Q}$  of the magnetic order. Therefore, besides the Nagaoka state, long-range magnetic order is ubiquitous for the studied systems. Next, we analyze the magnetic

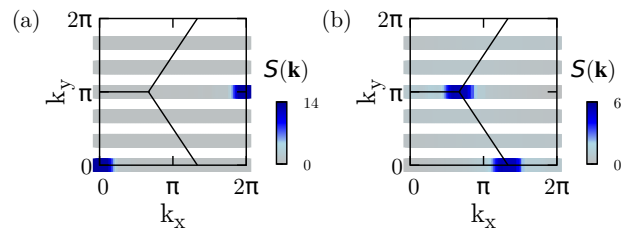


FIG. 4. Intensity plot of  $\mathcal{S}(\mathbf{k})$  for the triangular lattice with (a)  $t' = 0$ , and (b)  $t' = t$ . The solid lines indicate the edges of the hexagonal Brillouin zones. Notice the discreteness of  $k_y$  values.

pattern as a function of the kinetic energy frustrating hoppings  $t'$ .

First, we present the results for the triangular lattice. We have chosen the  $N = 54$  sites cluster for the presentation of  $\mathcal{S}(\mathbf{k})$  as, for  $L_y = 6$ , it is expected to be the cluster most representative of the two-dimensional case<sup>18</sup>. We begin revisiting the two previously known situations:  $t' = 0$  and  $t' = t$ . For  $t' = 0$ , Nagaoka’s theorem is valid and, consequently,  $\mathcal{S}(\mathbf{k})$  exhibits a sharp maximum at the magnetic wave vector  $\mathbf{Q} = \mathbf{0}$ , as it is shown in Fig. 4(a). The other known case,  $t' = t$ <sup>14</sup>, is presented in Fig. 4(b). We can see two  $\mathcal{S}(\mathbf{k})$  maxima at  $\mathbf{Q} = (\frac{4\pi}{3}, 0)$  and  $\mathbf{Q}^* = (\frac{2\pi}{3}, \frac{2\pi}{\sqrt{3}})$ , both equivalent and corresponding to the 120° Néel order.

Now, we analyze the magnetic order for intermediate  $t'$  between the two limits presented above. As long as  $t' < t'_c$ , we have found ferromagnetic order, that is  $\mathbf{Q} = \mathbf{0}$ , in agreement with the ground state energy analysis of the previous section. Increasing  $t'$  beyond the critical value, the  $\mathcal{S}(\mathbf{k})$  peak locates at  $\mathbf{Q} = (Q, 0)$ , with  $Q$  changing monotonously from  $Q = 0$  at  $t' = t'_c$  to  $Q = \frac{4\pi}{3}$  at  $t' = t$ , as it is shown in Fig. 5. This magnetic

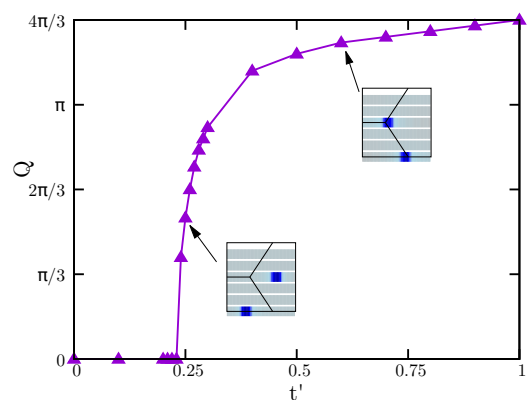


FIG. 5. Spiral pitch  $Q$  as a function of  $t'$  for the triangular lattice. Insets: intensity plots of  $\mathcal{S}(\mathbf{k})$  for  $t' = 0.25$  and  $0.6$ . The darker regions correspond to the magnetic wave vector  $\mathbf{Q} = (Q, 0)$  (and other equivalent point).

wave vector is characteristic of a spiral order with a pitch angle  $Q$  in the  $x$  direction, and it connects the ferromag-

netic and the  $120^\circ$  Néel orders. From the figure, it seems that  $Q$  depends continuously on  $t'$ , although it exhibits a sharp rise close to  $t'_c$ . For small spiral pitch, the period of the spin pattern along the  $x$  direction ( $\sim \frac{2\pi}{Q}$ ) can exceed the cluster length  $L_y$  ( $Q \lesssim \frac{\pi}{4}$  in our case), preventing a correct description of the spiral order. A clear manifestation of this kind of finite size effects is that, very close to the transition, the peaks of the magnetic structure factor are not so pronounced. For these reasons, we can not state categorically that the transition from the Nagaoka state to the spiral one is continuous, although the  $Q$  dependence on  $t'$  suggest it. To underline this point, it is worth remembering that, in the previous section, we have seen the ground state energy for the triangular lattice also behaves rather smooth across the transition. We can speculate that an infinite-order phase transition takes place here, like the one found as a function of doping, for  $t' = 0$ , in Ref.<sup>7</sup>.

From Fig. 5 we notice that, due to the sharp rise of  $Q$ , the spiral order has a pervasive antiferromagnetic character ( $Q \gtrsim \pi$ ), except near the transition point.

In the following, we focus on the square lattice model. In Figs. 6(a) and 6(b) we show the  $t' = 0$  and  $t' = t$  intensity plot of  $\mathcal{S}(\mathbf{k})$ , respectively. We have chosen the  $N = 60$  cluster in this case<sup>18</sup>. We can see in Fig. 6(a) that the ground state has ferromagnetic order, as it was expected, because of the validity of Nagaoka's theorem for  $t' = 0$ . For  $t' = t$ , Fig. 6(b) indicates that the ground state has the typical Néel order with magnetic wave vector  $\mathbf{Q} = (\pi, \pi)$ , as was found in Ref.<sup>14</sup>. The magnetic order evolution with second-nearest neighbor hopping  $t'$  is very simple. Below  $t'_c$  the ground state is the Nagaoka ferromagnet, while for  $t' > t'_c$  it is the  $\mathbf{Q} = (\pi, \pi)$  Néel order. Therefore, the transition is clearly discontinuous, with no intermediate order between the  $\mathbf{Q} = (0, 0)$  Nagaoka and  $\mathbf{Q} = (\pi, \pi)$  Néel states. It should be remember that, in this case, the ground state energy (Fig. 3) exhibits an appreciable non-analytical behavior at the transition. Similar discontinuous transitions occur when kinetic frustration is due to staggered magnetic fluxes<sup>12</sup>. Summarizing, the addition of rather small  $t'$  hoppings

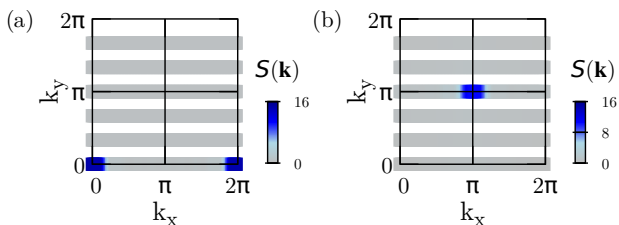


FIG. 6. Intensity plot of  $\mathcal{S}(\mathbf{k})$  for the square lattice with (a)  $t' = 0$ , and (b)  $t' = t$ . Solid lines refer to the edges of the square Brillouin zones.

( $t'/t \gtrsim 0.22$ ) destabilizes the Nagaoka state and it induces long-range antiferromagnetic order, whose characteristics depend on the system: a spiral pattern in the triangular lattice, and the usual Néel order in the square

case. Concerning the physical origin of this kinetic antiferromagnetism, recently we identified its microscopic mechanism<sup>14</sup>. While the introduction of  $t'$  increases the hole kinetic energy (the only one involved for  $U = \infty$ ) in a ferromagnetic background, quantum interference effects can release this kinetic energy frustration if the hole moves along a certain antiferromagnetic pattern. This release can occur in two different ways, depending on the lattice geometry and the hopping terms: (a) the hole acquires a non-trivial spin Berry phase due to the antiferromagnetic texture or, (b) the magnetic order leads to an effective vanishing of the hopping amplitude along the frustrating loops. In our work, the spin-Berry phase mechanism is operating for the stabilization of the spiral order in the triangular lattice model since, in that order, the hole acquires a  $\pi$  phase when it hops along one elementary triangle. On the other hand, for the square case, the effective hole nearest-neighbor hopping amplitude vanishes as a consequence of the antiparallel spin structure of the  $(\pi, \pi)$  Néel order, and the hole moves only along the diagonal directions. We refer the reader to Ref.<sup>14</sup> (especially to the Supplemental Material), for a more detailed discussion of the kinetic antiferromagnetism mechanism.

### C. Local magnetization

Finally, we have calculated the magnetic order parameter, that is, the local staggered magnetization  $M_s$ , which can be defined as

$$M_s = \sqrt{\frac{1}{N^2} \sum_{\alpha} \left\langle \left( \sum_{i \in \alpha} \mathbf{S}_i \right)^2 \right\rangle},$$

where  $\alpha$  denotes the magnetic sublattices. A straightforward calculation shows that  $M_s = \sqrt{\frac{\mathcal{S}(\mathbf{Q})}{N}}$ . On the other hand, for non-collinear magnetic structures, like the  $\mathbf{Q} = (Q, 0)$  spiral, we use the relation  $M_s = \sqrt{\frac{2\mathcal{S}(\mathbf{Q})}{N}}$ , that can be deduced considering semi-classical spin correlations,  $\langle \mathbf{S}_i \cdot \mathbf{S}_j \rangle \simeq M_s^2 \cos \mathbf{Q} \cdot (\mathbf{R}_j - \mathbf{R}_i)$ , for  $i \neq j$ .

The same procedure recovers  $M_s = \sqrt{\frac{\mathcal{S}(\mathbf{Q})}{N}}$  for collinear orders. The curve with open triangles (squares) in Fig. 7 shows the evolution of the local magnetization with  $t'$ , for the  $N = 54$  ( $N = 60$ ) triangular (square) cluster. The behavior for other clusters is qualitatively similar. In the Nagaoka phase,  $M_s$  takes the classical value, given by  $M_s^{clas} = \frac{1}{2} - \frac{1}{2N}$ , as it was expected for a fully saturated state. On the other hand, the kinetic antiferromagnetic phases have large values of  $M_s$ , especially the triangular model (upper panel of the figure) where it is close to  $M_s^{clas}$  for all  $t'$ .

In Ref.<sup>14</sup>, we found that, for the particular value  $t' = t$  and both models,  $M_s$  extrapolates to its classical value in the thermodynamic limit. There, we argued that the classical value is not reached for finite clusters due to

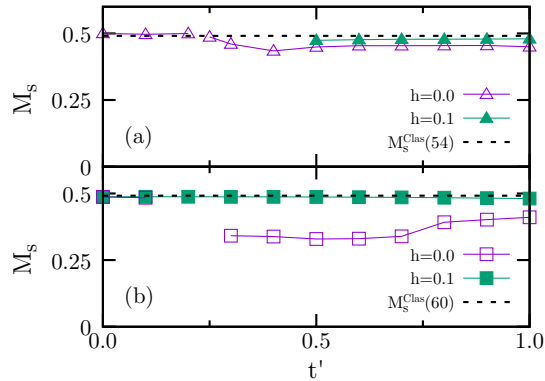


FIG. 7. Local magnetization  $M_s$  as a function of  $t'$  for (a) the  $N = 54$  triangular lattice without a magnetic field (open triangles) and with a magnetic field  $h = 0.1$  applied to one  $120^\circ$  sublattice (solid triangles); (b) the  $N = 60$  square lattice without a magnetic field (open squares) and with a magnetic field  $h = 0.1$  applied to one of the two sublattices of the  $(\pi, \pi)$  Néel order. The dashed lines correspond to the classical local magnetization,  $M_s^{clas} = \frac{1}{2} - \frac{1}{2N}$ .

the  $SU(2)$  symmetry of the Hubbard model. One way to confirm this idea, for commensurate magnetic orders, was the finding that the application of a small uniform magnetic field  $\vec{h} = h\hat{e}_z$ , in one sublattice only, was enough to pin the classical order for the finite clusters<sup>18</sup>.

In this work, we wonder if the remarkable classical character mentioned above extends to other values of  $t'$ . Hence, we have applied a magnetic field  $h = 0.1$  in one of the two (three) sublattices of the  $180^\circ$  ( $120^\circ$ ) structure in the square (triangular) lattice model. Notice that, in the triangular case, due to the incommensuration of the  $\mathbf{Q} = (Q, 0)$  spiral phase for a generic  $Q$ , the application of the pinning magnetic field matches the order only when  $Q \simeq \frac{4\pi}{3}$  (so, for  $t'/t \lesssim 0.5$  we do not apply  $h$ ). The curves with solid symbols in Fig. 7 show the  $t'$  dependence of  $M_s$  with the magnetic field  $h$  applied. Convincingly, it can be seen that  $h$  brings out the “hidden” classical nature of the kinetic antiferromagnetism in these finite clusters. Therefore, we have found that, for all  $t'$ , the ground state of the considered  $U = \infty$  Hubbard models has classical magnetism. Above  $t'_c$ , this is a remarkable result as it can be thought as a perfect counterpart of Nagaoka’s theorem. About the physical reason for the classical nature of the antiferromagnetism, we speculate that the hole motion under the  $U = \infty$  condition generates effective long-range spin interactions, that may favor classical ordering<sup>14,19</sup>.

#### IV. CONCLUSION

To conclude, we have investigated the evolution of the Nagaoka state with  $t'$  hopping processes that induce hole

kinetic energy frustration. To this purpose, the numerical density matrix renormalization group is used to compute the magnetic ground state properties of the  $U = \infty$  Hubbard model, with one hole doped away from half-filling, on two lattices: the spatially anisotropic triangular lattice and the square lattice with second-nearest neighbor hoppings.

We have found that the Nagaoka ferromagnetic state is destabilized for rather small frustrating hoppings:  $t'_c/t = 0.222$  ( $0.214$ ) for the triangular (square) lattice. Taking into account that these values are comparable to the corresponding ones for a simple 4-site cluster, we can state that Nagaoka physics is driven mainly by quantum interferences generated by the hole motion along the smallest lattice loops.

The analysis of the magnetic structure factor indicates that the ground state of the  $U = \infty$  Hubbard model has long-range magnetic order for all hopping  $t'$ . For  $t' > t'_c$ , the square lattice ground state has a classical  $(\pi, \pi)$  Néel order. In the triangular case, the magnetic order is a classical spiral pattern with magnetic wave vector  $\mathbf{Q} = (Q, 0)$ , that seems to connect continuously the Nagaoka ferromagnet at  $t' = t'_c$  with the  $120^\circ$  Néel antiferromagnet at the isotropic point  $t' = t$ .

Therefore, the kinetic antiferromagnetism, first discovered by Haerter and Shastry<sup>13</sup> on the triangular lattice and further developed by us<sup>14</sup>, seems to be a robust phenomenon in kinetically frustrated electronic systems. Its classical nature makes this antiferromagnetism the perfect counterpart of the Nagaoka’s state for frustrated systems. On the other hand, the lattice geometry affects the nature of the transition between the different classical states, as we have seen: continuous for the triangular lattice, discontinuous for the square one.

Finally, it remains a challenge to find experimental realizations of both, the old Nagaoka ferromagnetism and the new kinetic antiferromagnetism that have been studied in this and previous works<sup>14</sup>. Up to date, there is no clear evidence of Nagaoka physics in condensed matter systems, being the main obstacle the large onsite Coulomb repulsion needed,  $U/t \gtrsim 100$ . However, tunable Feshbach resonances in ultracold atoms allow to reach such large  $U$ ’s, and, on the other hand, the generation of artificial gauge fields in triangular optical lattices<sup>20</sup> can induce frustrated motion. Other proposals involve artificial lattice of quantum dots<sup>21</sup>, and high-density two-dimensional electron gas at the interface between Mott and band insulators<sup>22</sup>. All this opens the interesting possibility to test experimentally our proposals about kinetic magnetism.

#### ACKNOWLEDGMENTS

This work was supported by CONICET-PIP1060, and from CONICET-PIP0389.

- 
- <sup>1</sup> Y. Nagaoka, Phys. Rev. **147**, 392 (1966).
  - <sup>2</sup> E. Müller-Hartmann, Th. Hanisch, and R. Hirsch, Physica B **186-188**, 834 (1993).
  - <sup>3</sup> P. Fazekas, *Electron Correlation and Magnetism* (World Scientific, Singapore, 1999).
  - <sup>4</sup> H. Park, K. Haule, C. A. Marianetti, and G. Kotliar, Phys. Rev. B, **77**, 035107 (2008).
  - <sup>5</sup> L. Liu, H. Yao, E. Berg, S. R. White, and S. A. Kivelson, Phys. Rev. Lett. **108**, 126406 (2012).
  - <sup>6</sup> S. Liang and H. Pang, Europhys. Lett. **32**, 173 (1995).
  - <sup>7</sup> G. Carleo, S. Moroni, F. Becca, and S. Baroni, Phys. Rev. B, **83**, 060411 R, (2011)
  - <sup>8</sup> E. Eisenberg, R. Berkovits, D. A. Huse, and B. L. Altshuler, Phys. Rev. B **65**, 134437 (2002).
  - <sup>9</sup> A. M. Olés and P. Prelovsek, Phys. Rev. B **43**, 13348 (1991).
  - <sup>10</sup> W. Barford and J. H. Kim, Phys. Rev. B **43**, 559 (1991).
  - <sup>11</sup> J. Merino, B. J. Powell, and R. H. McKenzie, Phys. Rev. B **73**, 235107 (2006).
  - <sup>12</sup> Y. F. Wang, C.D. Gong, and Z. D. Wang, Phys. Rev. Lett. **100**, 037202 (2008).
  - <sup>13</sup> J. O. Haerter and B. S. Shastry, Phys. Rev. Lett. **95**,087202 (2005).
  - <sup>14</sup> C. N. Sposetti, B. Bravo, A. E. Trumper, C. J. Gazza, and L. O. Manuel, Phys. Rev. Lett. **112**, 187204 (2014).
  - <sup>15</sup> S. R. White, Phys. Rev. Lett. **69**, 2863, (1992).
  - <sup>16</sup> S. R. White and D. A. Huse, Phys. Rev. B **48**, 3844 (1993).
  - <sup>17</sup> W. F. Brinkman and T. M. Rice, Phys. Rev. B **2**, 1324 (1970).
  - <sup>18</sup> S. R. White and A. L. Chernyshev, Phys. Rev. Lett. **99**, 127004 (2007).
  - <sup>19</sup> E. Lieb and D. Mattis, J. Math. Phys. **3**, 749 (1962).
  - <sup>20</sup> J. Struck, C. Ölschläger, R.L. Targat, P. Soltan-Panahi, A. Eckardt, M. Lewenstein, P. Windpassinger, and K. Sengstock, Science **333**, 996 (2011).
  - <sup>21</sup> L. Gaudreau, S. A. Studenikin, A. S. Sachrajda, P. Zawadzki, A. Kam, J. Lapointe, M. Korkusinski, and P. Hawrylak, Phys. Rev. Lett. **97**, 036807 (2006).
  - <sup>22</sup> J. Iaconis, H. Ishizuka, D. N. Sheng, and L. Balents, Phys. Rev. B **93**, 155144 (2016).